Size-dependent two-photon excitation spectroscopy of CdSe nanocrystals

Mark E. Schmidt, Sean A. Blanton, Margaret A. Hines, and Philippe Guyot-Sionnest
James Franck Institute, 5640 South Ellis Avenue, University of Chicago, Chicago, Illinois 60637
(Received 27 November 1995)

Two-photon excitation spectra of highly monodisperse colloidal CdSe nanocrystals with sizes ranging from 22 to 43 Å are compared to one-photon excitation data and to a spherically confined effective-mass model. The main experimental features are well described by this model. However, the first one-photon and two-photon transitions appear indistinguishable, though the model predicts a 20-meV splitting. This discrepancy may reflect the sensitivity of the band-edge structure to deviations from the assumed spherical symmetry. [S0163-1829(96)03820-9]

Semiconductor nanocrystals exhibit interesting size-tuneable optical properties, due to the confinement of electronic wave functions,[1,2] have received much attention both for the insight they provide into the evolution of material properties as the crystal size passes from the molecular to the macroscopic limits[3] and for their possible uses in optical technologies.[4] For example, the figure of merit for all-optical switching is determined by the ratio of the nonresonant nonlinear refractive index to the two-photon absorption coefficient.[5] Calculations[6] and measurements[6–8] indicating that this figure of merit is enhanced in semiconductor nanocrystals compared to bulk semiconductors have recently been disputed.[9,10] This dispute can be addressed by coordinating a detailed linear and nonlinear spectroscopic study of well-characterized monodisperse samples with the development of theoretical models, which can successfully predict the effect of quantum confinement on the optical properties of the nanocrystals. Recent linear optical measurements,[11,12] performed on highly monodisperse colloidal CdSe (Ref. 13), have been convincingly modeled with an effective-mass theory, which includes spherical confinement, valence-band degeneracy, and nonparabolicity of the conduction band.[14–17] Previous two-photon spectroscopy studies were performed on rather polydisperse semiconductor doped glasses CdS (Ref. 18) and $CdS_{1-x}Se_x$ (Refs. 19 and 20). The study reported here on highly monodisperse CdSe colloids represents a significant improvement in spectroscopic detail and resolution and is a step towards a definitive assessment of the nonlinear optical properties of nanocrystals.

As discussed by several authors,[14–17] electron and hole wave functions in semiconductor nanocrystals are products of envelope wave functions and unit-cell basis functions. The unit-cell basis functions are constructed from Cd *s* orbitals and Se *p* orbitals ($p_{3/2}$ and $p_{1/2}$) for the conduction and valence bands, respectively. For spherical confinement geometry, the electron or hole wave functions are labeled by the total angular momentum F, its projection M, and the lowest angular momentum of the constitutive envelope spherical harmonics. For example, with the Luttinger parameters applicable to CdSe and in the size ranges studied here, the lowest hole state is $1S_{3/2}$, and the next state, $1P_{3/2}$, is predicted to lie about 20 meV higher in energy. For the conduction band, the electron states have total angular momentum $F=L\pm 1/2$ and the F label is dropped in the notation $1S_e$, $1P_e$, $1D_e$, $2S_e$, and so forth. Parity is also a good quantum number. The one-photon transitions satisfy selection rules $\Delta L=0,\pm 2$ and $\Delta F=0,\pm 1$ and the two-photon transitions satisfy $\Delta L=\pm 1,\pm 3$ and $\Delta F=0,\pm 1,\pm 2$. Therefore, one-photon and two-photon spectroscopies access completely separate manifolds of transitions.

After synthesis, purification and size-selective precipitation,[13,21] the CdSe nanocrystals have a narrow size distribution ($<10\%$). Further size selection is achieved by detecting fluorescence in several narrow ranges (4-nm bandwidth) on the blue edge of the fluorescence spectrum.[22] The nanocrystals are suspended in a glass forming mixture of diethyl ether, isopentane, and ethanol, injected into a 1.5-nm path length cuvette and cooled to 5 K in a helium vapor cryostat. A grating-tuned picosecond optical parametric source is used for excitation (continuous tuning from 1.65 to 1 eV, 25 Hz, 6 ps, ≈ 30 μJ, 10-meV bandwidth). For directly comparable one-photon excitation measurements, the output of the parametric source is doubled in a KDP crystal. The beam is focused into the glass sample with a 10-cm focal length lens, and the collected fluorescence is dispersed in a double monochromator. A portion of the excitation beam is split off prior to the sample and detected by either a pyroelectric detector or a photodiode for use as a calibrated reference. The one-photon excitation fluorescence signal is normalized by this reference signal. The two-photon excitation fluorescence signal is normalized by the square of this reference signal. Although this procedure does not normalize for variations in pulse width or focusing that occur as the parametric source is tuned, we expect these variations to be limited.

Two-photon fluorescence excitation spectra at 5 K are shown in Fig. 1 for each of five different nanocrystal samples. These samples had average nanocrystal diameters of 43, 39, 32, 29, and 22 Å as determined by a comparison with published one-photon absorption spectra.[13] As shown in Figs. 1 and 2(a), the two-photon spectra are highly structured, evolve with crystal size, and are markedly different from one-photon excitation spectra. To extract peak positions, the spectra are fitted to a sum of four to seven Gaussians. The combined excitation and detection resolution is ≈ 20 meV and the overall fit reproducibility on the position of the second and third fitted features is about ± 20 meV.

In Fig. 3, the energies of the first three fitted Gaussians are displayed as a function of the first one. The lines in this figure represent transitions predicted by the spherical con-

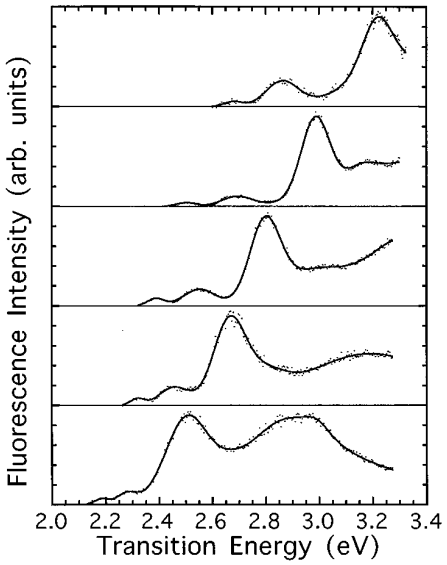

FIG. 1. Two-photon fluorescence excitation spectra at 5 K for five nominal sizes: 43, 39, 32, 29, and 22 Å. The spectra are offset for clarity and the lines are least-square fits, as described in the text.

finement model, which includes valence-band degeneracy, an infinite hole barrier, and a finite electron barrier, and are plotted as a function of the $1P_{3/2}$-$1S_e$ transition. The parameters used are the same ones shown by Norris and Bawendi[12] to provide the best agreement with the one-photon transitions. These parameters are the Luttinger parameters $\gamma_1 = 2.04$ and $\gamma = 0.58$, an electron barrier height of 8.9 eV, and simple Coulomb corrections $-1.8e^2/\varepsilon r$ for S/S pair states and $-1.7e^2/\varepsilon r$ for P/P pair states, where r is the radius of the particle.[17] The Coulomb correction for the S/P pairs should be $-0.94e^2/\varepsilon r$, but, in the following, we use the same correction as for S/S pairs. This can amount to a 70-meV difference over the range of sizes studied. These Coulomb corrections are not rigorous, since they neglect valence-band degeneracy, but they are reasonably correct and scale as $1/r$, which is sufficient for our purpose. We note that the Coulomb corrections have been treated more thoroughly within this simple model.[23]

In Fig. 3, the solid lines (a), (b), and (d),[12] correspond to $1S_{3/2}$-$1S_e$, $2S_{3/2}$-$1S_e$, and $1P_{3/2}$-$1P_e$, respectively. The dashed lines are the lowest-energy two-photon transitions and it is apparent that several assignments are compatible with the second and third features. While transitions with identical principal quantum numbers should be dominant for the case of nondegenerate bands and infinite well depths, this assumption is not valid in the present case. In order to assign the transitions, we have numerically calculated the transition probabilities for the one-photon and two-photon transitions[24] to $1S_e$ and $1P_e$ electron states[14,15]

$$P^{(n)}_{i\to f} = \frac{2\pi}{h} M^{(n)}_{if} g(nh\omega) E^{2n}, \quad n = 1,2 \tag{1}$$

where

$$M^{(1)}_{i,v\to f,c} = |\langle \Phi_{i,v} | \Phi_{f,c} \rangle \mu_K|^2, \tag{2}$$

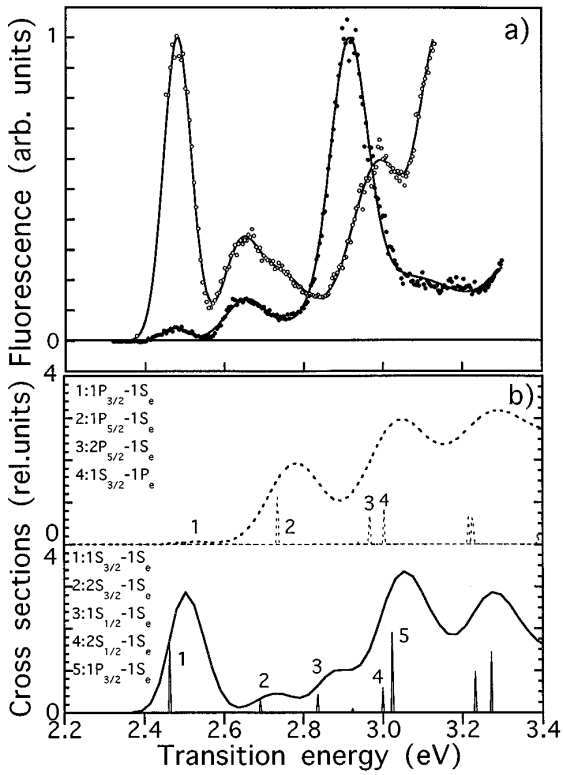

FIG. 2. (a) One-photon fluorescence excitation (open dots) and two-photon fluorescence excitation spectra (filled dots) for the sample of nominally 29-Å diameter nanocrystals with the fluorescence detected as 515 nm, at 5 K. The lines are least-square fits, as described in the text. (b) Simulated one-photon (solid line) and two-photon (dashed line) excitation spectra for a distribution of 32 ± 1 Å^2 spherical CdSe particles. Absolute cross sections are obtained by multiplying the vertical scale by 1.7×10^{-46} cm^4 s^{-1} (two photon) and 2.2×10^{-15} cm^2 (one photon).

$$M^{(2)}_{i,v\to f,c} = \left| \sum_{s,v} \frac{\langle \Phi_{i,v}|er|\Phi_{s,v}\rangle\langle \Phi_{s,v}|\Phi_{f,c}\rangle \mu_K}{h(\omega - \omega_{si})} + \sum_{s,c} \frac{\mu_K \langle \Phi_{1,v}|\Phi_{s,c}\rangle\langle \Phi_{s,c}|er|\Phi_{f,c}\rangle}{h(\omega - \omega_{si})} \right|^2,$$

E is the electric field, Φ denotes the envelope wave functions, and μ_K is the unit-cell transition moment obtained from the Kane parameter[14] for CdSe ($\mu_K = 21\times10^{-18}$ esu). Interband one-photon transitions involve only the overlap between the initial valence state $\Phi_{i,v}$ and the final conduction state $\Phi_{f,c}$, while interband two-photon transitions involve products of intraband and interband transition dipole moments. For qualitative comparison, two-photon and one-photon spectra are simulated using a Gaussian broadening with a variance $\sigma_E/(E - Eg) = 5\%$ reflecting an effective size distribution $\sigma_R/R \approx 2.5\%$. In addition, the widths are increased in linear relation to the overall degeneracy of the transition. This is then convoluted with an asymmetric fluorescence emission simulating the experimentally observed LO-phonon progression. As can be seen in Fig. 2(b), this procedure provides a qualitative agreement for the first transitions of the one-photon experimental data. Although the strength of the $2S_{3/2}$-$1S_e$ transition is noticeably weaker in the calculation than in the experiment for all sizes calculated,

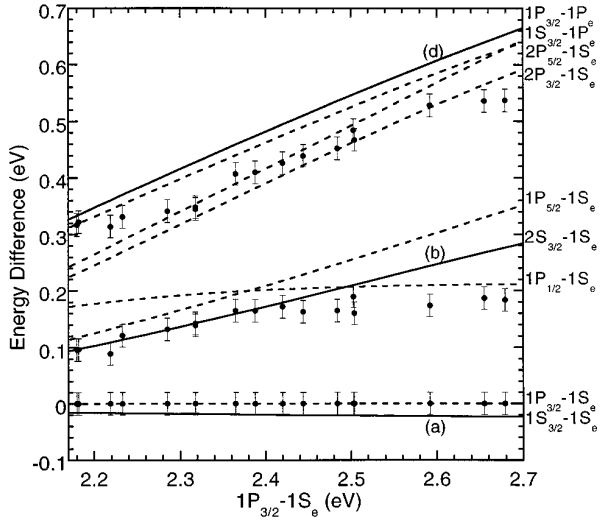

FIG. 3. Measured energy of the two-photon transitions at 5 K (solid dot), as a function of the first transition energy. The lines are the calculated one-photon (solid lines) and two-photon (dashed lines) transition energies after substracting the $1P_{3/2}$-$1S_e$ transition.

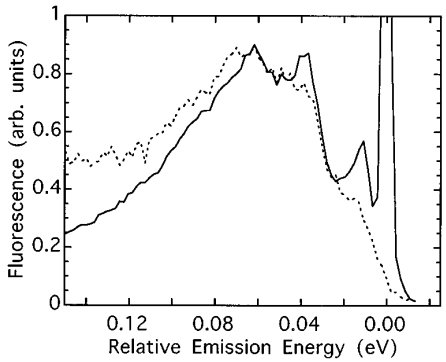

FIG. 4. Dispersed fluorescence spectra at 5 K, with excitation at 532 nm (2.33 eV) and resolution of 0.6 nm, solid line; and at 1064 nm (1.164 eV), with a resolution of 3 nm, dashed line. The spike at zero energy for one-photon excitation is the 532-nm laser line.

one should keep in mind that the fluorescence quantum yield may be different for different initial excited states. For the two-photon spectra, the summations in Eq. (1) have been performed over all intermediate states of energies less than 2 and 5 eV for holes and electrons, respectively. As shown in Fig. 2(b), the simulated two-photon spectrum obtained from the cross sections is in qualitative agreement with the observations. The $1P_{3/2}$-$1S_e$ transition is clearly the only possibility for the first transition and its weak strength is well reproduced by the simulations. The second feature in the calculation is completely dominated by $1P_{5/2}$-$1S_e$, rather than by $1P_{1/2}$-$1S_e$, but it is too large by a factor of ≈ 3 compared to the experimental data. Also, its predicted energy deviates from the experimental observation for the smaller particles as seen in Fig. 3. The third feature appears to be composed of both $2P_{5/2}$-$1S_e$ and $1S_{3/2}$-$1P_e$ and the predicted energies are fairly well described as a function of size. Therefore, for the general features, the main discrepancy is that the contribution from the $P_{5/2}$ states is systematically too large for all the sizes of nanocrystal studied here. Nevertheless, given the simplicity of the model, the qualitative differences between the one-photon and two-photon spectra are quite satisfactorily explained.

As could be expected, this simple description appears insufficient in finer detail and, in particular, at the band edge. As noted earlier, the $1P_{3/2}$-$1S_e$ transition is predicted to lie at least 20 meV higher in energy than the $1S_{3/2}$-$1S_e$ transition. This prediction is incorrect. A comparison of the one-photon and two-photon excitation spectra shown in Fig. 2(a) reveals that there is less than a 20-meV shift between the first peaks in the two spectra. To improve on the estimate of the shift, we performed dispersed fluorescence measurements using the narrow-band excitation of the Nd:YAG fundamental (two-photon excitation) and its second harmonic (one-photon excitation). Assuming identical recombination mechanisms and a single-particle size, the energy difference between the first one-photon and two-photon transitions should appear in the different Stokes shifts of the fluorescence. Size inhomogeneity will prevent this observation, except if one excites on the red edge of the distribution leading to fluorescence line narrowing. As shown in Fig. 4, the Stokes shift is identical for the two cases even though the clearly visible LO phonon progression indicates that only a narrow class of nanocrystals is excited. Accordingly, the first two-photon and one-photon transitions are experimentally indistinguishable and we estimate that if there is any shift, it must be less than 5 meV or $\frac{1}{5}$ of the LO-phonon spacing and within the homogeneous linewidths. Consequently, the lowest nanocrystal transition does not show a definite parity. This is an important observation that will affect the understanding of the recombination dynamics in these nanocrystals, which has so far been discussed only in terms of trapping[25] or in terms of the fine structure of the $1S_{3/2}$ state.[26]

The failure of the model to correctly describe the band edge may indicate a mixing of the $1S_{3/2}$ and $1P_{3/2}$ hole states or a splitting of the components of these states into two broad multiplets which overlap. Refinements to the model could include improved Coulomb corrections,[23] exchange interactions,[26] surface polarization effects,[27] and deviation from spherical symmetry.[28] The Coulomb attraction, which is weaker for $1P_{3/2}$-$1S_e$ than for $1S_{3/2}$-$1S_e$, should increase even further the energy difference between the two transitions, while the exchange interaction should be a weak effect. In addition, neither the Coulomb nor the exchange interaction will mix these pair states of opposite parity.

The spherical model also neglects the C_{3v} symmetry of the unit cell, which lifts the degeneracy of the atomiclike $p_{3/2}$ orbitals and leads to the A-B splitting between the heavy and light holes at the zone center ($\Delta = 26$ meV). From the first-order perturbation theory, the resulting splitting between states with $|M| = \frac{3}{2}$ and $|M| = \frac{1}{2}$ has been estimated to be between 0.2Δ and Δ for $1S_{3/2}$ (Ref. 28) and a similar splitting can be expected for the $1P_{3/2}$ state.

The shape of the particle can also deviate from spherical symmetry to ellipsoidal (prolate or oblate) or hexagonal (faceted D_{6h} symmetry). These perturbations conserve parity and will not lead to mixing, but they will lead to splitting of states of angular momentum larger than $\frac{1}{2}$ into the different symmetry classes. For ellipsoidal deviations, the central position of a multiplet will not shift,[29] but the $P_{3/2}$ splitting should be larger than the $S_{3/2}$ splitting, since the latter is zero to first order in the deformation in the absence of valence-band degeneracy.[30]

Finally, mixing of $P_{3/2}$ and $S_{3/2}$ will occur only for perturbations that do not conserve parity. In the wurtzite nanocrystal, the inversion symmetry is broken in the unit cell and, therefore, the one-photon and two-photon selection rules can no longer be mutually exclusive. However, the relative cross sections may still be very different. To estimate this effect, we consider the permanent dipole moment μ_c of the unit cell and the intraband transition dipole moment μ_i of the delocalized wave function. We use $\mu_c \approx 10^{-19}$ esu, which was calculated by a pseudopotential method for wurtzite ZnS (Ref. 31). Typically, we can expect μ_i/e to be a fraction of the nanocrystal radius. If the average potential is still spherically symmetric, then the two-photon cross section for transitions allowed in zero order should be stronger than for transitions forbidden in zero order by a factor $(\mu_i/\mu_c)^2$. Thus, this intrinsic breaking of inversion symmetry should remain a small effect. Indeed, for 32-Å diameter nanocrystals, the ratio of the two-photon transition probabilities of the nominally forbidden $1S_{3/2}$-$1S_e$ to the allowed $1P_{3/2}$-$1S_e$ is calculated to be 3×10^{-4}. A stronger effect can be present if the nanocrystal is polar, as may happen when faces have different terminations. This will produce an electric field, likely along the c axis, that will couple the S and P manifolds of hole states. When the states are nearly degenerate, as for $1S_{3/2}$ and $1P_{3/2}$, a small perturbation can lead to complete mixing. As an estimate, the polarity of the unit cell leads to an internal electric field $E=\mu_c/V_c/(2\varepsilon_{\text{matrix}}+\varepsilon_{\text{CdSe}})\approx 60$ esu. Using the transition element $\langle 1P_{3/2,3/2}|z|1S_{3/2,3/2}\rangle = 3.9$ Å, calculated for a nanocrystal of 32-Å diameter, the field-induced interaction between the two states is then 0.7 meV. This is much too small to induce significant mixing. We note that the corresponding dipolar surface charge $Q=r^2\mu_c/(4V_c)$ is only $\approx 0.01e$, which is also quite small. It may be that larger fields are present in the colloidal nanocrystals. This internal field is related to the permanent dipole moment, which has not been experimentally observed as yet.

In conclusion, the assignments of the dominant two-photon transitions in the CdSe nanocrystals are, in order of increasing energy, $1P_{3/2}$-$1S_e$, $1P_{5/2}$-$1S_e$, and $2P_{5/2}$-$1S_e$ or $1S_{3/2}$-$1P_e$. A model that includes spherical confinement, valence-band degeneracy, and nonparabolicity of the electron and hole bands is inaccurate at the band edge, since it fails to predict that the lowest two-photon transition is experimentally indistinguishable from the lowest one-photon transition. This may indicate state splitting due to deviation from spherical symmetry or mixing due to crystal polarity, and it will have consequences for the recombination dynamics. However, the main qualitative features of the two-photon excitation spectra are quite successfully reproduced and this is an indication that the other nonlinear optical properties of the nanocrystals will also be successfully modeled.

We thank M. G. Bawendi for making available the one-photon data (Ref. 12) prior to publication. This work was supported in part by the MRSEC program of NSF under Grant No. DMR-9400379. We also gratefully acknowledge support from the David and Lucille Packard Foundation.

[1] Al. L. Efros and A. L. Efros, Fiz. Tekh. Poluprovodn. **16**, 1209 (1981) [Sov. Phys. Semicond. **16**, 772 (1982)].
[2] L. E. Brus, J. Chem. Phys. **80**, 4403 (1984).
[3] M. G. Bawendi, M. L. Steigerwald, and L. E. Brus, Annu. Rev. Phys. Chem. **41**, 477 (1990).
[4] Y. Wang, Acc. Chem. Res. **24**, 133 (1991).
[5] V. Mizrahi, K. W. DeLong, G. I. Stegeman, M. A. Saifi, and M. J. Andrejco, Opt. Lett. **14**, 1140 (1989).
[6] D. Cotter, M. G. Burt, and R. J. Manning, Phys. Rev. Lett. **68**, 1200 (1992).
[7] D. C. Rogers, R. J. Manning, B. J. Ainslie, D. Cotter, M. J. Yates, J. M. Parker, and S. Morgan, IEEE Phot. Tech. Lett. **6**, 1017 (1994).
[8] M. D. Dvorak, B. L. Justus, and A. D. Berry, Opt. Commun. **116**, 149 (1995).
[9] G. P. Banfi, V. Degiorgio, and J. M. Tan, J. Opt. Soc. Am. B **12**, 621 (1995).
[10] G. B. Banfi, V. Degiorgio, D. Fortusini, and H. M. Tan, Appl. Phys. Lett. **67**, 13 (1995).
[11] D. J. Norris, A. Sacra, C. B. Murray, and M. G. Bawendi, Phys. Rev. Lett. **72**, 2612 (1994).
[12] D. J. Norris and M. G. Bawendi, Phys. Rev. B (to be published).
[13] C. B. Murray, D. J. Norris, and M. G. Bawendi, J. Am. Chem. Soc. **115**, 8706 (1993).
[14] A. I. Ekimov, F. Hache, M. C. Schanne-Klein, D. Richard, C. Flytzanis, I. A. Kudryavtsev, T. V. Yazeva, A. V. Rodina, and Al. L. Efros, J. Opt. Soc. Am. B **10**, 100 (1993).
[15] G. B. Grigoryan, E. M. Kazaryan, Al. L. Efros, and T. V. Yazeva, Fiz. Tverd. Tela (Leningrad) **32**, 1772 (1990) [Sov. Phys. Solid State **32**, 1031 (1990)].
[16] J. B. Xia, Phys. Rev. B **40**, 8500 (1989).
[17] P. C. Sercel and K. J. Vahala, Phys. Rev. B **42**, 3690 (1990).
[18] K. I. Kang, B. P. McGinnis, Sandalphon, Y. Z. Hu, S. W. Koch, N. Peyghambarian, A. Mysyrowicz, L. C. Liu, and S. H. Risbud, Phys. Rev. B **45**, 3465 (1992).
[19] R. Tommasi, M. Lepore, M. Ferrara, and I. M. Catalano, Phys. Rev. B **46**, 12 261 (1992).
[20] R. Tommasi, M. Lepore, and I. M. Catalano, Solid State Commun. **85**, 539 (1993).
[21] J. E. Bowen Katari, V. L. Colvin, and A. P. Alivisatos, J. Phys. Chem. **98**, 4109 (1994).
[22] M. G. Bawendi, W. L. Wilson, L. Rothberg, P. J. Carroll, T. M. Jedju, M. L. Steigerwald, and L. E. Brus, Phys. Rev. Lett. **65**, 1623 (1990).
[23] G. T. Einevoll, Phys. Rev. B **45**, 3410 (1992).
[24] For example, Y. R. Shen, *The Principles of Nonlinear Optics* (Wiley, New York, 1984).
[25] M. G. Bawendi, P. J. Carroll, W. L. Wilson, and L. E. Brus, J. Chem. Phys. **96**, 946 (1992).
[26] M. Nirmal, D. J. Norris, M. Kuno, M. G. Bawendi, Al. L. Efros, and M. Rosen, Phys. Rev. Lett. **75**, 3728 (1995).
[27] L. Banay, P. Gilliot, Y. Z. Hu, and S. W. Koch, Phys. Rev. B **45**, 14 136 (1992).
[28] Al. L. Efros, Phys. Rev. B **46**, 7448 (1992).
[29] Al. L. Efros and A. V. Rodina, Phys. Rev. B **47**, 10 005 (1993).
[30] L. D. Landau and E. M. Lifshitz, *Quantum Mechanics*, 3rd ed. (Pergamon, Oxford, 1977), p. 137.
[31] M. L. Cohen and J. R. Chelikowsky, *Electronic Structure and Optical Properties of Semiconductors* (Springer-Verlag, Berlin, 1989).